Original Article

MiR-148a-3p attenuates apoptosis and inflammation by targeting *CNTN4* in atherosclerosis

Kai Wang[1], Xi-Tong Huang[2], Yan-Ping Miao[3], Xiao-Long Bai[3], Feng Jin[3]

[1]Department of Neurosurgery, The Affiliated Hospital of Inner Mongolia Medical University, Hohhot, China; [2]Department of Traditional Chinese Medicine, China Pharmaceutical University, Nanjing, China; [3]Department of Radiology, The Affiliated Hospital of Inner Mongolia Medical University, Hohhot, China

Contributions: (I) Conception and design: F Jin, K Wang; (II) Administrative support: None; (III) Provision of study materials or patients: None; (IV) Collection and assembly of data: K Wang, XT Huang, YP Miao, XL Bai; (V) Data analysis and interpretation: YP Miao, XL Bai; (VI) Manuscript writing: All authors; (VII) Final approval of manuscript: All authors.

Correspondence to: Feng Jin. Department of Radiology, The Affiliated Hospital of Inner Mongolia Medical University, Hohhot 010050, China. Email: doctorjinfeng@nmgfy.com

Background: Atherosclerosis (AS) seriously affects human health. The role of microRNAs (miRNAs) in the pathogenesis and progression of AS has become a focus of research. Our goal was to identify the biological effect of differentially expressed miRNAs (DE-miRNAs) in AS.

Methods: To analyze differentially expressed genes (DEGs), including differentially expressed mRNAs (DE-mRNAs) and DE-miRNAs, in AS by using the Gene Expression Omnibus (GEO) database and limma package. DEGs protein-protein interaction (PPI) network and functional enrichment analysis were constructed by using the search tool for the retrieval of interacting genes/proteins (STRING) database, Cytoscape software and Cytoscape plugin "ClueGO2.5.6". We established a coexpression network of dysregulated miRNAs and mRNAs to predict the function of miRNAs by using miRWalk database and Pearson correlation coefficient (PCC) analysis. Cellular experiments were used to validate the results of bioinformatics.

Results: First, 69 common DEGs were obtained from datasets GSE43292 and GSE97210 using the limma package in R. Next, a DEG PPI network was constructed. Functional enrichment analysis of DEGs showed that 11 functional pathways were significantly enriched, such as positive regulation of monocyte chemotaxis. Seven common DE-miRNAs were obtained from the GSE99685 dataset and DE-mRNAs predicted miRNAs through the miRWalk database. The miRNA-mRNA network constructed using Cytoscape software suggested that *miR-148a-3p* targeted contactin 4 (*CNTN4*). Quantitative real-time polymerase chain reaction (qRT-PCR) assay results indicated that *miR-148a-3p* was downregulated and *CNTN4* was upregulated in the THP-1 + phorbol 12-myristate 13-acetate (PMA) + oxidized low-density lipoprotein (oxLDL) group compared with the THP-1 + PMA group. qRT-PCR, flow cytometry, and enzyme-linked immunosorbent assay (ELISA) found that upregulated *miR-148a-3p* significantly inhibited the expression of *CNTN4*, cell apoptosis, and interleukin-6 (IL-6) and tumor necrosis factor-alpha (TNF-α) concentrations in oxLDL-induced THP-1 macrophages. In addition, a dual-luciferase reporter assay demonstrated that *CNTN4* was a target gene of *miR-148a-3p*.

Conclusions: Overall, these findings suggested that *miR-148a-3p* inhibited oxLDL-induced cell apoptosis and inflammation via targeting *CNTN4* in THP-1 macrophages.

Keywords: Atherosclerosis (AS); *miR-148a-3p*; *CNTN4*; apoptosis; inflammation

Submitted Jun 23, 2022. Accepted for publication Oct 18, 2022.
doi: 10.21037/atm-22-3768
View this article at: https://dx.doi.org/10.21037/atm-22-3768

© Annals of Translational Medicine. All rights reserved.

Introduction

Atherosclerosis (AS) is the main cause of cardiovascular diseases, including coronary heart disease, cerebral infarction, and peripheral vascular disease (1). It is also a systemic disease with immune components, triggering an inflammatory response and angiogenesis and vessel narrowing, ultimately leading to plaque instability and thrombosis (2-4). AS has a high incidence and disability rate and seriously threatens human health, especially for elderly people (5). Therefore, finding the molecular mechanism of AS is important for prevention, diagnosis, and treatment.

With the development of microarray and RNA sequencing (RNA-seq) technology, research on differentially expressed genes (DEGs) between diseases and normal tissues has improved our understanding of the molecular mechanisms of different diseases (6). To improve the standard of early diagnosis and treatment in AS, it is crucial to identify biomarkers and understand their molecular functions. Mounting evidence has shown that the analysis of DEGs could help identify important biomarkers (7,8), which can provide more opportunities for personalized treatment. MicroRNAs (miRNAs) are involved in the physiological functions and molecular mechanisms of AS by regulating the expression of DEGs (9). In AS, *miR-181a-5p* inhibits vascular inflammation and nuclear factor (NF)-κB activation by targeting *TAB2* (10). A Previous study has reported that *miR-155* promotes the oxidized low-density lipoprotein (oxLDL)-induced activation of NLRP3 inflammasomes in THP-1 macrophages by regulating the extracellular signal-regulated kinase (ERK1/2) pathway (11). These findings are helpful for achieving a better understanding of the functional mechanism and clinical development of AS.

Here, we analyzed DEGs in AS and then performed a series of bioinformatics analyses and cell experiments to identify and verify the genes closely related to the onset of AS as therapeutic targets. We started with the function of DEGs and then constructed an miRNA-messenger RNA (mRNA) coexpression network. Next, we found AS-related miRNAs and predicted their targeted genes. Cellular experiments were used to validate the results of bioinformatics. The identification of biomarkers in AS can help achieve the goals of prevention and early diagnosis in AS. We present the following article in accordance with the MDAR reporting checklist (available at https://atm.amegroups.com/article/view/10.21037/atm-22-3768/rc).

Methods

Data acquisition

The study was conducted in accordance with the Declaration of Helsinki (as revised in 2013). The high throughput sequencing dataset (GSE99685) for AS and 2 microarray datasets (GSE43292 and GSE97210) were downloaded from the Gene Expression Omnibus (GEO) database. GSE43292 included 32 atheroma plaques and 32 normal tissues. GSE97210 consisted of 6 samples, including 3 AS samples and 3 normal samples. GSE99685 contained miRNA expression profiles of 3 controls and 3 which had been oxLDL-stimulated for 48 hours, resulting in foam cell formation.

DEGs between AS and normal tissue

The limma package in R was used to find DEGs in AS compared with normal samples (12). An absolute value of log2|fold change (FC)| ≥1 and P value ≤0.05 were used as the criteria for differentially expressed mRNAs (DE-mRNAs) and miRNAs (DE-miRNAs).

Construction of DEG protein-protein interaction (PPI) network

The PPI network was constructed using the search tool for the retrieval of interacting genes/proteins (STRING) database and visualized by Cytoscape software (version v3.7.2, https://cytoscape.org/), which is a useful tool for analysis and visualization of molecular interaction networks.

Functional enrichment analysis of DEGs

The Cytoscape plugin "ClueGO2.5.6" was used for signaling pathway enrichment analysis, with P value <0.05 regarded as statistically significant.

Construction of coexpression network of common DE-miRNAs and DE-mRNAs

The DE-mRNAs predicted miRNAs through the miRWalk database. Based on Pearson correlation coefficient (PCC) analysis, we established a coexpression network of dysregulated miRNAs and mRNAs to predict the function of miRNAs. PCC >0.9 and P value <0.01 were regarded

© Annals of Translational Medicine. All rights reserved.

Table 1 Specific primers used for qRT-PCR analysis

Gene name	Sequence
GAPDH	F: GGAGCGAGATCCCTCCAAAAT
	R: GGCTGTTGTCATACTTCTCATGG
CNTN4	F: AACGCAGAGCTTAGTGTTATAGC
	R: TTTGGAGACGCTTTTGGCTTA
U6	F: GGGCCATGCTAATCTTCTCTGTA
	R: CAGGTCCAGTTTTTTTTTTTTTT
MiR-148a-3p	F: GGTCAGTGCACTACAGAACTTTG
	R: GATGATGATAAGCAAATGCTGACTGAAC

qRT-PCR, quantitative real-time polymerase chain reaction; *GAPDH*, glyceraldehyde 3-phosphate dehydrogenase; *CNTN4*, contactin 4.

statistically significant. Cytoscape software (13) was then used to construct the coexpression network.

Cell culture

THP-1 cell line was obtained from American Type Culture Collection (ATCC, Rockville, MD, USA). The cells were maintained in Roswell Park Memorial Institute 1640 (RPMI-1640) supplemented with 10% fetal bovine serum (FBS) and 1% penicillin/streptomycin solution in a 37 ℃ humidified 5% CO_2 incubator. The THP-1 cells were incubated with 100 nM phorbol 12-myristate 13-acetate (PMA) for 72 hours for differentiation into macrophage cells. The THP-1 macrophages were then induced by 100 μg/mL oxLDL into foam cell formation.

Cell transfection

The *miR-148a-3p* mimics were synthesized by Generay Biotech Shanghai Co., Ltd. (China). The oxLDL-induced THP-1 macrophages were transfected with *miR-148a-3p* mimics or negative control and Lipofectamine 3000 for 48 hours.

Cell apoptosis assay

The cell apoptosis rate was analyzed by flow cytometry. Briefly, after transfection, cells were washed with phosphate-buffered saline (PBS) and analyzed using an Annexin V-FITC kit. The cells were incubated with Annexin V in the dark for 15 minutes. Next, propidium iodide (PI) was added to the cells for 5 minutes in the dark. The stained cells were then detected by a flow cytometer.

Enzyme-linked immunosorbent assay (ELISA)

Interleukin-6 (IL-6) and tumor necrosis factor-α (TNF-α) were analyzed using ELISA kits (Proteintech, Wuhan, China) according to the manufacturer's instructions.

Quantitative real-time PCR (qRT-PCR)

Total RNA was extracted from the THP-1 macrophages using TRIzol reagent (Invitrogen, Waltham, MA, USA). Subsequently, total RNA was synthesized to complementary DNA (cDNA) by TaqMan reverse transcription kit. To quantify the mRNA level of *miR-148a-3p* and contactin 4 (*CNTN4*), 2 μL cDNA was amplified using TaqMan miRNA quantification kit with the ABI PRISM 7500 Sequence Detection System. The qPCR amplification conditions were: 95 ℃ for 10 minutes, 45 cycles of 95 ℃ for 45 seconds, and 60 ℃ for 30 seconds. Glyceraldehyde 3-phosphate dehydrogenase (*GAPDH*) or *U6* was normalized as an internal control. The relative quantification was determined using the $2^{-\Delta\Delta Ct}$ method. The primer sequences are shown in *Table 1*.

Dual-luciferase reporter assay

The sequences targeting 3'UTR of *CNTN4* [wild type (WT): TCTGCAATGCACTGAAGACA, mutated type (MUT): TCTGCAAACAGACCGAGACA] were cloned into the pGL3 vector. The pGL3-*CNTN4* 3'UTR WT and pGL3-*CNTN4* 3'UTR MUT were synthesized by GenePharma (Shanghai, China). The oxLDL-induced THP-1 macrophages cells were cotransfected with 20 nM *miR-148a-3p* mimics and 0.2 μg pGL3-*CNTN4* 3'UTR WT or pGL3-*CNTN4* 3'UTR MUT using Lipofectamine 2000. After 48 hours, the luciferase activity was analyzed.

Statistical analysis

Data analysis was performed with GraphPad Prism 8.0. All experiments were performed at least 3 times. The data are expressed as mean ± standard error of mean (SEM). One-way analysis of variance (ANOVA) test or Student's *t*-test were used to determine statistical significance. P<0.05 was

© Annals of Translational Medicine. All rights reserved.

considered statistically significant.

Results

Identification of DEGs in AS

To explore changes at the gene transcription level of AS, we performed differential expression analyses between AS plaques and normal tissues. The "limma" R package was used to identify DEGs base on P value <0.05 and fold change ≥2. The volcano plot (*Figure 1A*) and heatmap (*Figure 1B*) for the AS group and normal group samples in dataset GSE97210 found 6,337 DE-mRNAs between the two groups. For the AS group and normal group samples in dataset GSE43292, the volcano plot (*Figure 1C*) and heatmap (*Figure 1D*) identified 112 DE-mRNAs between the two groups.

Functional enrichment analysis and construction of PPI network of common DEGs

The Venn diagram exhibited 69 common DE-mRNAs in the GSE43292 and GSE97210 datasets, including 35 upregulated DE-mRNAs and 34 downregulated DE-mRNAs (*Figure 2A*). To enhance the reliability of this research, we constructed a PPI network based on the DE-mRNAs of the 2 datasets. A network of the interactions between the DE-mRNAs was constructed using the STRING database and visualized by Cytoscape. The PPI network contained 28 upregulated DE-mRNAs and 16 downregulated DE-mRNAs (*Figure 2B*). In order to uncover the potential biological functions of the 69 common DE-mRNAs, we performed functional pathway and gene network enrichment analysis. The results showed that 11 functional pathways were significantly enriched, including positive regulation of monocyte chemotaxis, indolalkylamine metabolic process, circadian entrainment, extracellular matrix (ECM) disassembly, neurotransmitter biosynthetic process, ECM-receptor interaction, peroxisome proliferator-activated receptor (PPAR) signaling pathway, and negative regulation of intracellular transport, among others. The 27 DEGs, including *CD36*, *MMP* family, *TPH1*, and *CCR1*, among others, were significantly enriched for the 11 functional pathways (*Figure 2C*). Based on these results, we believed that DE-mRNAs played a crucial role in the progression of AS.

Identification of DE-miRNAs in oxLDL-induced macrophage cells and AS

We then identified DE-miRNAs related to AS. Firstly, we analyzed the DE-miRNAs in the GSE99685 dataset. Volcano plot analysis identified 154 DE-miRNAs based on |log2 (FC)|>1 and P<0.05, including 69 upregulated miRNAs and 85 downregulated miRNAs (*Figure 3A*). The heatmap in *Figure 3B* shows DE-miRNA expression in the GSE99685 dataset. The Venn diagram in *Figure 3C* shows that there are 7 common DE-miRNAs between the predicted miRNAs of the targeting DE-mRNAs and DE-miRNAs in GSE99685. To investigate the interaction between DE-miRNAs and DE-mRNAs, an miRNA-mRNA network was constructed (*Figure 3D*). A total of 7 miRNAs, including 5 downregulated miRNAs (*miR-92-2p*, *miR-205-5p*, *miR-31-5p*, *miR-148a-3p*, and *miR-222-3p*) and 2 upregulated miRNAs (*miR-26a-5p* and *miR-501-3p*), and 9 target genes (*SCRG1*, *NPNT*, *TTLL7*, *PLD5*, *THRB*, *FRK*, *CNTN4*, *MPP6*, and *GRIA1*) made up the miRNA-mRNA network.

MiR-148a-3p attenuates apoptosis and inflammation by targeting CNTN4 in oxLDL-induced THP-1 macrophages

Next, we analyzed the mRNA level of *miR-148-3p* and *CNTN4* in oxLDL-induced THP-1 macrophages. Compared with the THP-1 + PMA group, *miR-148a-3p* expression was significantly decreased and the level of *CNTN4* was significantly increased in the THP-1 + PMA + oxLDL group (*Figure 4A*). To elucidate the cell apoptosis and inflammation effect of *miR-148-3p* on oxLDL-induced THP-1 macrophages, the *miR-148-3p* mimics were transfected to model cells. qRT-PCR assay revealed that *miR-148-3p* expression was remarkably increased and *CNTN4* expression was remarkably decreased in the model + *miR-148a-3p* mimics group compared with the model group (*Figure 4B*). Upregulated *miR-148a-3p* decreased cell apoptosis in oxLDL-induced THP-1 macrophages (*Figure 4C*). In addition, the expression of IL-6 and TNF-α were significantly reduced in the model + *miR-148a-3p* mimics group compared with the model group (*Figure 4D*). To further ensure that *CNTN4* was the target gene of *miR-148a-3p*, luciferase activity assay showed that *miR-148a-3p* mimics inhibited the luciferase activity in oxLDL-induced THP-1 macrophages transfected with *CNTN4* WT

© Annals of Translational Medicine. All rights reserved.

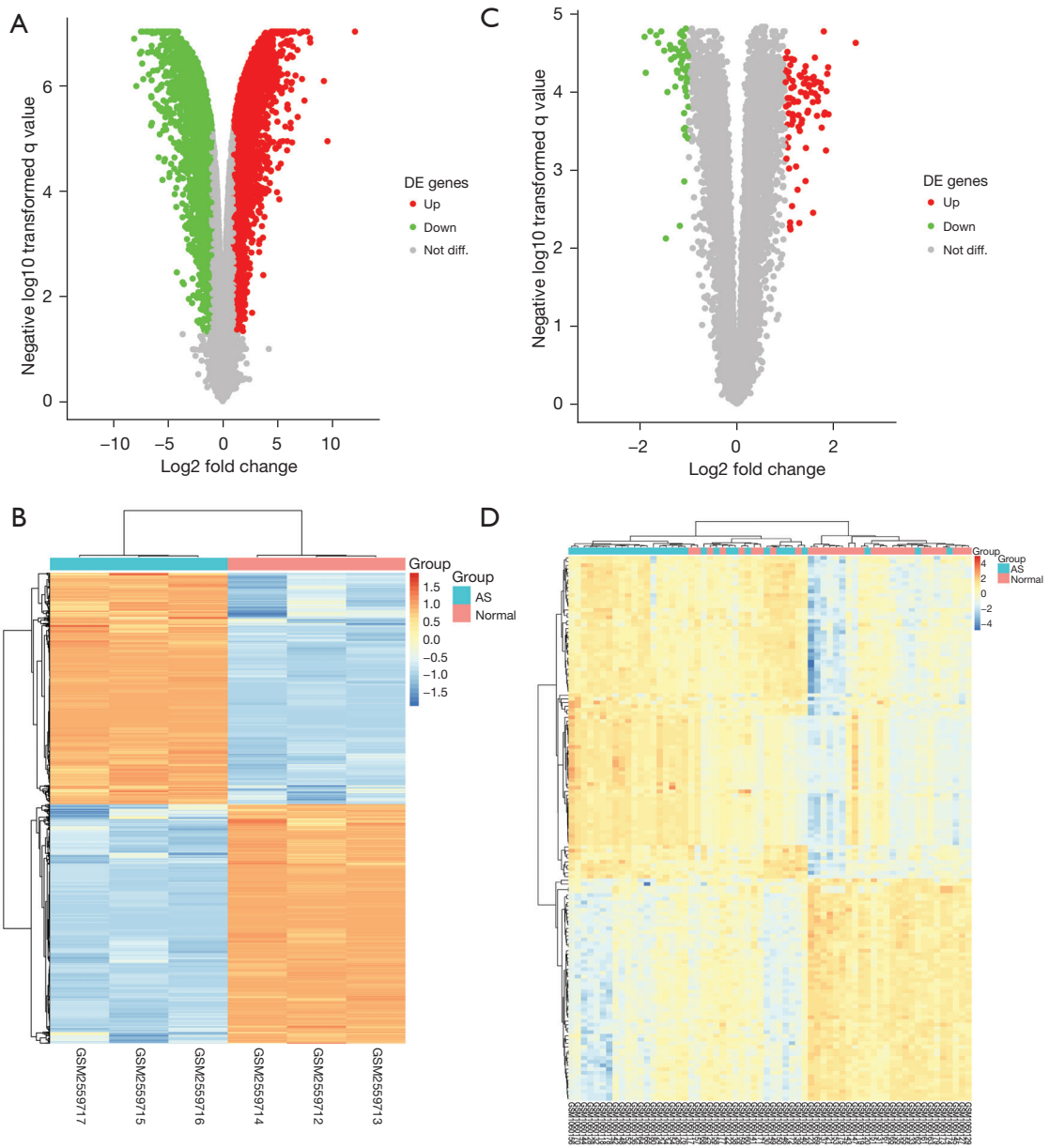

Figure 1 Identification of DE-mRNAs in AS. (A,B) Volcano plots (A) and heatmap (B) of the 6,337 DE-mRNAs associated with AS were analyzed by R software with the limma package loaded from datasets GSE97210. (C,D) Volcano plots (C) and heatmap (D) of the 112 DE-mRNAs associated with AS were analyzed by R software with the limma package loaded from datasets GSE43292. Red dots and green dots represent upregulated genes and downregulated genes with $|\log2FC| \geq 1$ and P value ≤ 0.05, respectively. Blue column represents AS group and red column represents normal group. DE-mRNAs, differentially expressed mRNAs; AS, atherosclerosis.

compared with oxLDL-induced THP-1 macrophages transfected with *CNTN4* MUT (*Figure 4E*).

Discussion

Previous studies have shown that DEGs were involved in the pathogenesis of AS (14,15). Meng *et al.* identified *TPM2* as a potential biomarker for the AS diagnosis and treatment (16). Huang *et al.* found 3 hub genes, including *KDELR3*, *CD55*, and *DYNC2H1*, which could be used as diagnostic and therapeutic biomarkers for AS (17). Here, we first identified 69 DE-mRNAs through the high throughput

© Annals of Translational Medicine. All rights reserved.

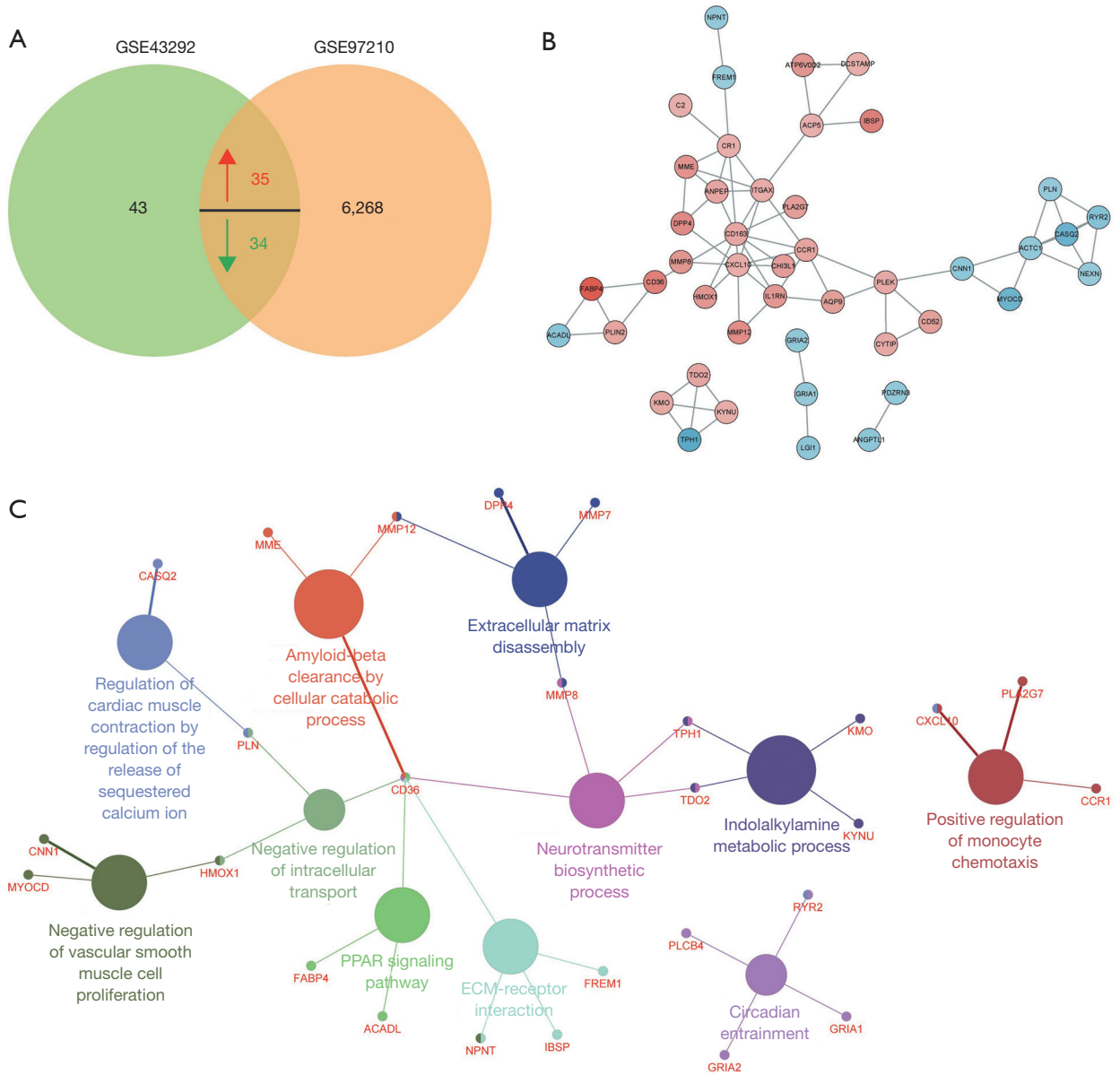

Figure 2 PPI network of common DE-mRNAs in GSE43292 and GSE97210. (A) Venn diagram represents that common DE-mRNAs in datasets GSE43292 and GSE97210. (B) PPI network of DE-mRNAs. The red circles and blue circles represent up-regulated and down-regulated DE-mRNAs, respectively. (C) Functional enrichment analysis was performed using Cytoscape. PPI, protein-protein interaction; DE-mRNAs, differentially expressed mRNAs.

sequencing dataset related to AS and normal vascular endothelial tissue. In order to have a better understanding of these differential genes, we performed functional pathway and gene network enrichment analysis, and 11 functional pathways were significantly enriched, including negative regulation of vascular smooth muscle cell (VSMC) proliferation, PPAR signaling pathway, and monocyte chemotaxis. The 27 DEGs, including *CD36*, *MMP* family, *TPH1*, and *CCR1*, were significantly enriched for the 11 functional pathways.

CD36 serves as a signaling hub protein at the crossroad of inflammation, fatty acid metabolism, and lipid metabolism (18,19). It has been reported that a lack of *CD36* inhibited the development of AS in CD36-deficient

© Annals of Translational Medicine. All rights reserved.

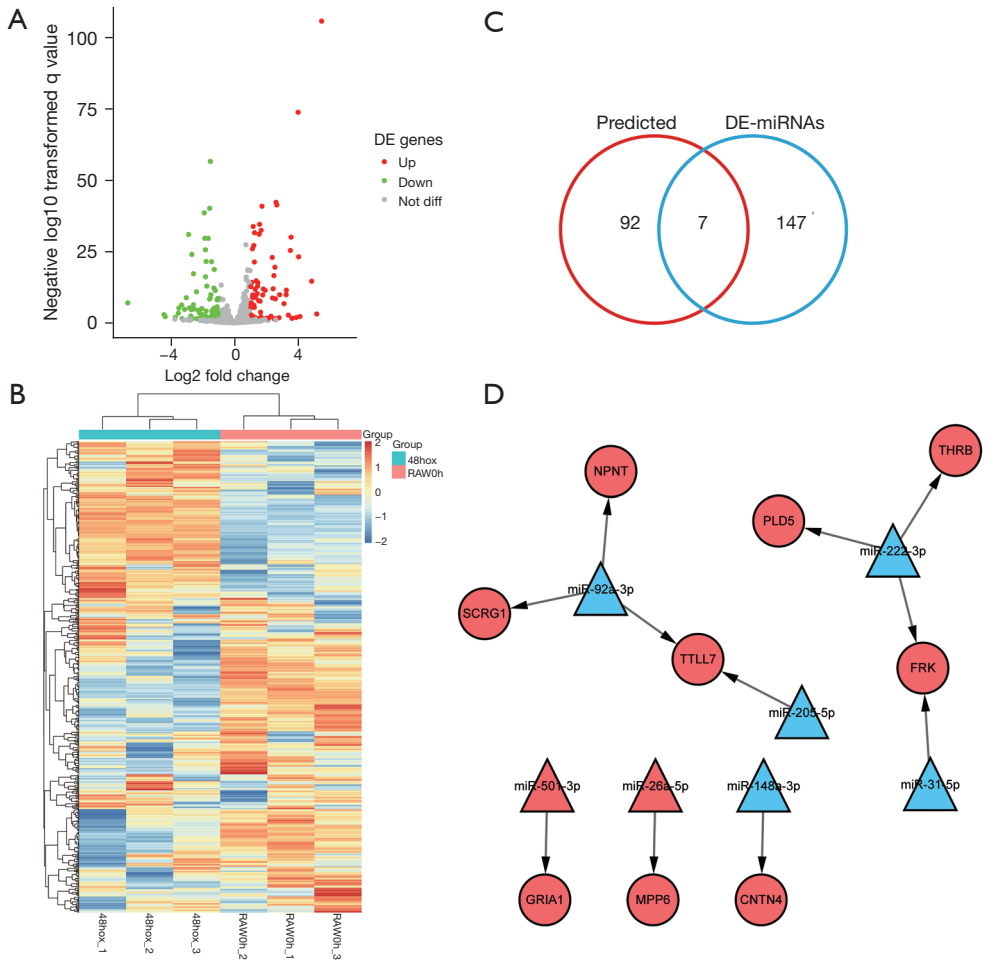

Figure 3 Identification of DE-miRNAs in AS. (A) Volcano plots of the 69 upregulated DE-miRNAs and 85 downregulated miRNAs in GSE99685 by R software with limma package based |log2FC|≥1 and P≤0.05. Red dots and green dots represent up-expressed and down-expressed genes, respectively. (B) The heatmap of the 69 up-regulated DE-miRNAs and 85 down-regulated miRNAs expression between the 48hox group and RAW0h group in GSE99685. 48hox group indicates oxLDL-stimulated RAW 264.7 cells; RAW0h group indicates RAW 264.7 cell control. Blue column represents 48hox group and red column represents RAW0h group. (C) The Venn diagram showing the 7 common DE-miRNAs in the predicted miRNA of the targeting DE-mRNAs and GSE99685. (D) The correlation between DE-miRNA and targeted genes were predicted by miRWalk and visualized by Cytoscape software. Red indicates upregulation and blue indicates downregulation. Circles represent DE-mRNAs and triangles represent DE-miRNAs. DE-miRNAs, differentially expressed miRNAs; AS, atherosclerosis; DE-mRNAs, differentially expressed mRNAs; oxLDL, oxidized low-density lipoprotein.

mice. Recent studies have reported the complex functions of *PPA*R as a therapeutic target during inflammation and lipid metabolism and energy homeostasis (20,21), while VSMC proliferation has been shown to significantly increase mortality and atherosclerotic plaque rupture in AS (22,23). A previous study suggested that *miR-146b-5p* suppressed VSMC proliferation and migration and atherosclerotic plaque formation in AS (24). Macrophages and monocyte chemotaxis are central to the development of AS (25). Function enrichment analyses confirmed that DE-mRNAs, whether up- or down-regulated genes, were involved the process of AS.

To date, the function of most dysregulated miRNAs in human diseases such as AS is still unclear (26). We know that miRNAs play a regulatory role on their co-expressed mRNAs. Hence, we established a coexpression miRNA-mRNA network to explore potential regulatory relationships. A total of 7 miRNAs, including 5

© Annals of Translational Medicine. All rights reserved.

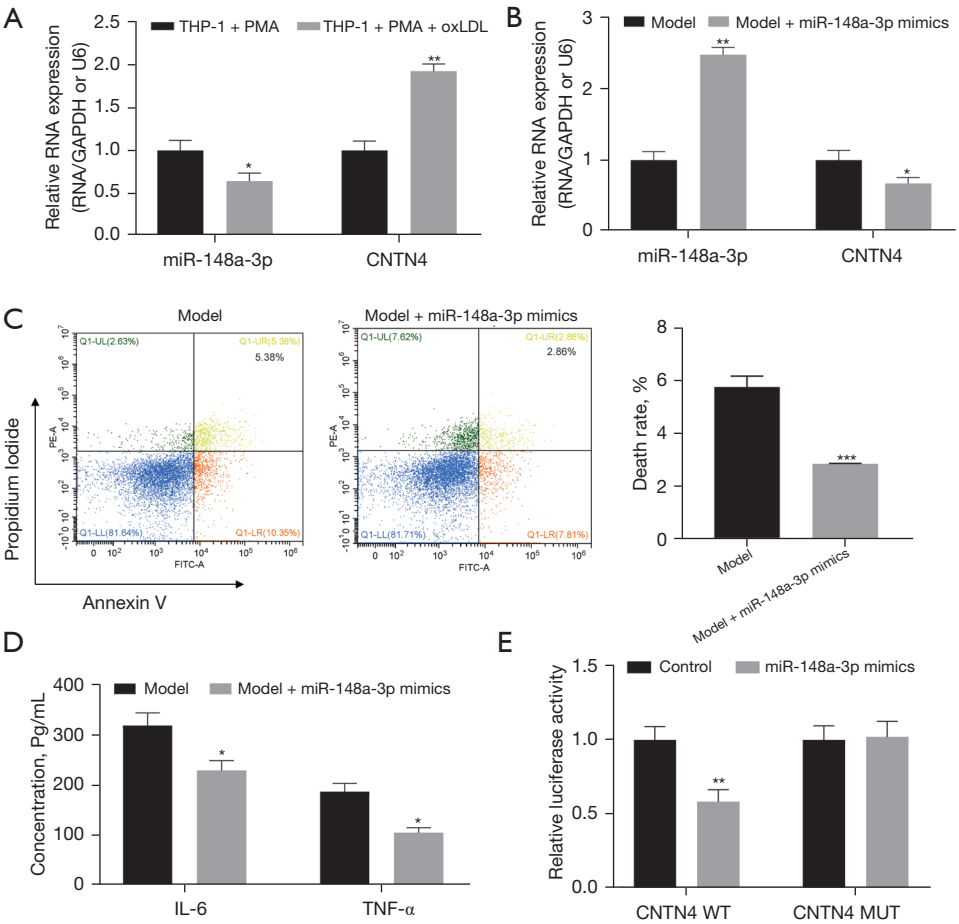

Figure 4 *MiR-148a-3p* suppresses apoptosis and inflammation in oxLDL induced THP-1 macrophages cells by targeting *CNTN4*. (A) qRT-PCR assay of *miR-148a-3p* and *CNTN4* in the THP-1 + PMA group and THP-1 + PMA + oxLDL group. (B) qRT-PCR assay detected the mRNA level of *miR-148a-3p* and *CNTN4* in the model and model + *miR-148a-3p* mimics groups. (C) Flow cytometry assay was performed to detect cell apoptosis. (D) ELISA assay was performed to detect IL-6 and TNF-α concentrations. (E) The dual-luciferase reporter assay was used to analyze the luciferase activity in the *CNTN4* WT and *CNTN4* MUT groups. Results are presented as the mean ± SEM, n=3. *, P<0.05; **, P<0.01 ***, P<0.001. oxLDL, oxidized low-density lipoprotein; *CNTN4*, Contactin 4; PMA, phorbol 12-myristate 13-acetate; qRT-PCR, quantitative real-time polymerase chain reaction; IL-6, interleukin-6; TNF-α, tumor necrosis factor alpha; WT, wild type; MUT, mutated type.

downregulated miRNAs (*miR-92-2p*, *miR-205-5p*, *miR-31-5p*, *miR-148a-3p*, and *miR-222-3p*) and 2 upregulated miRNAs (*miR-26a-5p* and *miR-501-3p*), and 9 target genes (*SCRG1*, *NPNT*, *TTLL7*, *PLD5*, *THRB*, *FRK*, *CNTN4*, *MPP6*, and *GRIA1*) made up the miRNA-mRNA network. AS is a lipid-driven inflammatory disease, and inflammation has long been considered a marker of AS. Recent studies have found that *miR-148a-3p* plays a critical role in inflammatory diseases (27-29) and angiogenesis (30,31). The knockdown of SULT2B1b has been shown to inhibit the inflammatory response via increasing the *miR-148a-3p* level in macrophages (32). Moreover, *CNTN4* was reported to be associated with the development of cardiovascular events (33).

The use of THP-1 cells as an AS model has been widely employed. In this study, THP-1 cells were induced with 100 nM PMA for 72 hours to differentiate into macrophage cells. The above studies found that oxLDL induced the inflammatory response. The THP-1 macrophages were then induced by 100 μg/mL oxLDL into foam cell formation. It has been reported that *miR-148a-3p* suppressed the expression of inflammatory factors

© Annals of Translational Medicine. All rights reserved.

in oxLDL-induced human umbilical vein endothelial cells (HUVECs) via targeting *KLF* (29). Here, we revealed that *miR-148a-3p* was markedly decreased and *CNTN4* expression level was markedly increased in the THP-1 + PMA + oxLDL group, and the overexpression of miR-148-3p remarkably increased the expression of *CNTN4* in oxLDL-induced THP-1 macrophages. In the functional experiment, *miR-148a-3p* inhibited cell apoptosis and IL-6 and TNF-α concentrations in oxLDL-induced THP-1 macrophages. To further confirm the mRNA target of *miR-148a-3p*, luciferase activity assay revealed that *miR-148a-3p* targeted *CNTN4*. Our results demonstrated that *miR-148a-3p* attenuated apoptosis and inflammation by targeting *CNTN4* in oxLDL-induced THP-1 macrophages.

Results of this study could help develop a better understanding of the pathogenesis of AS, and provide a new theoretical basis for the targeted therapy of AS inflammation and drug development. Follow-up experiments about whether the signaling pathways can be blocked by intervening with one or several miRNAs to inhibit or slow down the progression of AS are planned for the future.

Conclusions

In brief, our work provided a comprehensive analysis based on bioinformatics and cell function experiments showed that *miR-148a-3p* inhibited apoptosis and inflammation by targeting *CNTN4* in AS.

Acknowledgments

Funding: This work was supported by the Inner Mongolia Natural Science Foundation (No. 2018LH08046), Doctor Starting Fund of The Affiliated Hospital of Inner Mongolia Medical University (No. NYFYBS2018 to Feng Jin), National Natural Science Foundation of China (No. 81860558), Inner Mongolia Medical University Affiliated Hospital Doctor Fund Project (No. NYFYBS2018 to Kai Wang), General Project of Inner Mongolia Natural Science Foundation (No. 2018LH08040), and Inner Mongolia Medical University Science and Technology Million (Joint) Project (No. YKD2017KJBW (LH) 003).

Footnote

Reporting Checklist: The authors have completed the MDAR reporting checklist. Available at https://atm.amegroups.com/article/view/10.21037/atm-22-3768/rc

Data Sharing Statement: Available at https://atm.amegroups.com/article/view/10.21037/atm-22-3768/dss

Conflicts of Interest: All authors have completed the ICMJE uniform disclosure form (available at https://atm.amegroups.com/article/view/10.21037/atm-22-3768/coif). All authors report that this work was supported by the Inner Mongolia Natural Science Foundation (No. 2018LH08046), the National Natural Science Foundation of China (No. 81860558), the General project of the Inner Mongolia Natural Science Foundation (No. 2018LH08040), and the Inner Mongolia Medical University Science and Technology Million (Joint) Project (No. YKD2017KJBW (LH) 003). In addition, KW reports that this work was supported by the Inner Mongolia Medical University Affiliated Hospital Doctor Fund Project (No. NYFYBS2018) and FJ reports that this work was supported by the Doctor Starting Fund of the Affiliated Hospital of Inner Mongolia Medical University (No. NYFYBS2018). The authors have no other conflicts of interest to declare.

Ethical Statement: The authors are accountable for all aspects of the work in ensuring that questions related to the accuracy or integrity of any part of the work are appropriately investigated and resolved. The study was conducted in accordance with the Declaration of Helsinki (as revised in 2013).

Open Access Statement: This is an Open Access article distributed in accordance with the Creative Commons Attribution-NonCommercial-NoDerivs 4.0 International License (CC BY-NC-ND 4.0), which permits the non-commercial replication and distribution of the article with the strict proviso that no changes or edits are made and the original work is properly cited (including links to both the formal publication through the relevant DOI and the license). See: https://creativecommons.org/licenses/by-nc-nd/4.0/.

References

1. Pahwa R, Jialal I. Atherosclerosis. [Updated 2022 Jun 19]. In: StatPearls [Internet]. Treasure Island (FL): StatPearls Publishing; 2022 Jan. Available online: https://www.ncbi.nlm.nih.gov/books/NBK507799/
2. Jing L, Shu-Xu D, Yong-Xin R. A review: Pathological and molecular biological study on atherosclerosis. Clin Chim

© Annals of Translational Medicine. All rights reserved.

Acta 2022;531:217-22.
3. Comarița IK, Vîlcu A, Constantin A, et al. Therapeutic Potential of Stem Cell-Derived Extracellular Vesicles on Atherosclerosis-Induced Vascular Dysfunction and Its Key Molecular Players. Front Cell Dev Biol 2022;10:817180.
4. Camaré C, Pucelle M, Nègre-Salvayre A, et al. Angiogenesis in the atherosclerotic plaque. Redox Biol 2017;12:18-34.
5. Raposeiras-Roubin S, Rosselló X, Oliva B, et al. Triglycerides and Residual Atherosclerotic Risk. J Am Coll Cardiol 2021;77:3031-41.
6. Su W, Zhao Y, Wei Y, et al. Exploring the Pathogenesis of Psoriasis Complicated With Atherosclerosis via Microarray Data Analysis. Front Immunol 2021;12:667690.
7. de Yébenes VG, Briones AM, Martos-Folgado I, et al. Aging-Associated miR-217 Aggravates Atherosclerosis and Promotes Cardiovascular Dysfunction. Arterioscler Thromb Vasc Biol 2020;40:2408-24.
8. Chen H, Wang Y, Sun B, et al. Negative correlation between endoglin levels and coronary atherosclerosis. Lipids Health Dis 2021;20:127.
9. Churov A, Summerhill V, Grechko A, et al. MicroRNAs as Potential Biomarkers in Atherosclerosis. Int J Mol Sci 2019;20:5547.
10. Su Y, Yuan J, Zhang F, et al. MicroRNA-181a-5p and microRNA-181a-3p cooperatively restrict vascular inflammation and atherosclerosis. Cell Death Dis 2019;10:365.
11. Zheng B, Yin WN, Suzuki T, et al. Exosome-Mediated miR-155 Transfer from Smooth Muscle Cells to Endothelial Cells Induces Endothelial Injury and Promotes Atherosclerosis. Mol Ther 2017;25:1279-94.
12. Ritchie ME, Phipson B, Wu D, et al. limma powers differential expression analyses for RNA-sequencing and microarray studies. Nucleic Acids Res 2015;43:e47.
13. Choudhary K, Meng EC, Diaz-Mejia JJ, et al. scNetViz: from single cells to networks using Cytoscape. F1000Res 2021;10:eISCB Comm J-448.
14. Weinstock A, Rahman K, Yaacov O, et al. Wnt signaling enhances macrophage responses to IL-4 and promotes resolution of atherosclerosis. Elife 2021;10:67932.
15. Liu Y, Liu N, Liu Q. Constructing a ceRNA-immunoregulatory network associated with the development and prognosis of human atherosclerosis through weighted gene co-expression network analysis. Aging (Albany NY) 2021;13:3080-100.
16. Meng LB, Shan MJ, Qiu Y, et al. TPM2 as a potential predictive biomarker for atherosclerosis. Aging (Albany NY) 2019;11:6960-82.
17. Huang HM, Jiang X, Hao ML, et al. Identification of biomarkers in macrophages of atherosclerosis by microarray analysis. Lipids Health Dis 2019;18:107.
18. Rekhi UR, Omar M, Alexiou M, et al. Endothelial Cell CD36 Reduces Atherosclerosis and Controls Systemic Metabolism. Front Cardiovasc Med 2021;8:768481.
19. Lange NF, Graf V, Caussy C, et al. PPAR-Targeted Therapies in the Treatment of Non-Alcoholic Fatty Liver Disease in Diabetic Patients. Int J Mol Sci 2022;23:4305.
20. Christofides A, Konstantinidou E, Jani C, et al. The role of peroxisome proliferator-activated receptors (PPAR) in immune responses. Metabolism 2021;114:154338.
21. Chandra A, Kaur P, Sahu SK, et al. A new insight into the treatment of diabetes by means of pan PPAR agonists. Chem Biol Drug Des 2022. [Epub ahead of print]. doi: 10.1111/cbdd.14020.
22. Miano JM, Fisher EA, Majesky MW. Fate and State of Vascular Smooth Muscle Cells in Atherosclerosis. Circulation 2021;143:2110-6.
23. Grootaert MOJ, Finigan A, Figg NL, et al. SIRT6 Protects Smooth Muscle Cells From Senescence and Reduces Atherosclerosis. Circ Res 2021;128:474-91.
24. Sun D, Xiang G, Wang J, et al. miRNA 146b-5p protects against atherosclerosis by inhibiting vascular smooth muscle cell proliferation and migration. Epigenomics 2020;12:2189-204.
25. Feng X, Chen W, Ni X, et al. Metformin, Macrophage Dysfunction and Atherosclerosis. Front Immunol 2021;12:682853.
26. Zhao Z, Sun W, Guo Z, et al. Mechanisms of lncRNA/microRNA interactions in angiogenesis. Life Sci 2020;254:116900.
27. Zhang J, Xu X, Huang X, et al. Analysis of microRNA expression profiles in porcine PBMCs after LPS stimulation. Innate Immun 2020;26:435-46.
28. Ma D, Zhang Y, Chen G, et al. miR-148a Affects Polarization of THP-1-Derived Macrophages and Reduces Recruitment of Tumor-Associated Macrophages via Targeting SIRPα. Cancer Manag Res 2020;12:8067-77.
29. Wang F, Ge J, Huang S, et al. KLF5/LINC00346/miR-148a-3p axis regulates inflammation and endothelial cell injury in atherosclerosis. Int J Mol Med 2021;48:152.
30. Zhang P, Lu B, Zhang Q, et al. LncRNA NEAT1 Sponges MiRNA-148a-3p to Suppress Choroidal Neovascularization and M2 macrophage polarization. Mol Immunol 2020;127:212-22.
31. Ge H, Shrestha A, Liu C, et al. MicroRNA 148a-3p

© Annals of Translational Medicine. All rights reserved.

promotes Thrombospondin-4 expression and enhances angiogenesis during tendinopathy development by inhibiting Krüppel-like factor 6. Biochem Biophys Res Commun 2018;502:276-82.
32. Yin M, Lu J, Guo Z, et al. Reduced SULT2B1b expression alleviates ox-LDL-induced inflammation by upregulating miR-148-3P via inhibiting the IKKβ/NF-κB pathway in macrophages. Aging (Albany NY) 2021;13:3428-42.
33. McCarthy NS, Vangjeli C, Surendran P, et al. Genetic variants in PPARGC1B and CNTN4 are associated with thromboxane A2 formation and with cardiovascular event free survival in the Anglo-Scandinavian Cardiac Outcomes Trial (ASCOT). Atherosclerosis 2018;269:42-9.

Cite this article as: Wang K, Huang XT, Miao YP, Bai XL, Jin F. *MiR-148a-3p* attenuates apoptosis and inflammation by targeting *CNTN4* in atherosclerosis. Ann Transl Med 2022;10(22):1201. doi: 10.21037/atm-22-3768

© Annals of Translational Medicine. All rights reserved.